INL/EXT-16-40231-Revision-0

Quarterly Management Document FY16, 4th Quarter, Physics-based Creep Simulations of Thick Section Welds in High Temperature and Pressure Applications

Thomas M. Lillo, Wen Jiang

October 2016

The INL is a U.S. Department of Energy National Laboratory
operated by Battelle Energy Alliance

INL/EXT-16-40231-Revision-0

Quarterly Management Document FY16, 4th Quarter, Physics-based Creep Simulations of Thick Section Welds in High Temperature and Pressure Applications

Thomas M. Lillo, Wen Jiang

October 2016

Idaho National Laboratory
Idaho Falls, Idaho 83415

http://www.inl.gov

Prepared for the
U.S. Department of Energy
Office of Fossil Energy
Under DOE Idaho Operations Office
Contract DE-AC07-05ID14517

Quarterly Management Document – FY16, 4th Quarter, Physics-based Creep Simulations of Thick Section Welds in High Temperature and Pressure Applications

Document # INL/EXT-16-40231

WBS Element	Project Title	Contract Number	Contract Start	Contract End
C.B.10.02.02.40	Physics-based Creep Simulations of Thick Section Welds in High Temperature and Pressure Applications	FEAA90	06/01/15	09/30/2016

Performer Name and Address	Principal Investigator(s)
Thomas Lillo Idaho National Laboratory P.O. Box 1625 Idaho Falls, ID 83415	Thomas Lillo

BUDGET AND COST REPORT

Prior Year Funds ($K)				**148**								
Total Current Year Commitment ($K)				**398**								
Projected Current Year Costs ($K)				**305**								
	O	**N**	**D**	**J**	**F**	**M**	**A**	**M**	**J**	**J**	**A**	**S**
Planned Costs	**34**	**34**	**80.4**	**25**	**25**	**25**	**25**	**32**	**21**	**22**	**22**	**22**
Actual Costs	**40.2**	**81.9**	**17.0**	**3.5**	**0**	**32**	**42**	**16**	**27**	**31**	**30**	**23**
Variance	**-6.2**	**-47.9**	**63.4**	**21.5**	**25**	**-7.0**	**-17**	**-16**	**-6**	**-9**	**-8**	**-1**

MILESTONE REPORT

Milestone Designation	Milestone Description	Due Date	Revised Due Date	Completion Date
A	Evaluate current MOOSE capabilities	09/30/2015		09/30/2015
B	Complete Alloy 617 weld characterization	10/30/2015		11/18/2015
C	Receipt of Alloy 740H plates	10/30/2015		11/05/2015
D	Complete welds in Alloy 740H	11/16/2015	7/31/2016	7/31/2016
E	Characterize Alloy 740H welds	02/01/2016	09/30/2016	9/02/2016
F	Creep model development – Stage 1	09/30/2016		9/30/2016

TECHNICAL HIGHLIGHTS

Milestone D, "Welding procedure development"

The narrow weld groove design used in the initial weld qualification effort was redesigned and now resembles a more convention wide-groove design, Fig. 1. This design has been used extensively at INL in welding of ni-based alloys, specifically Alloy 617. Three welded plates with this weld groove design were completed by the end of July and then subjected to the post-weld heat treatment (800ºC for 4 hrs). Fabrication of both cross weld and all-weld metal creep specimens is expected to occur in the first quarter of FY17.

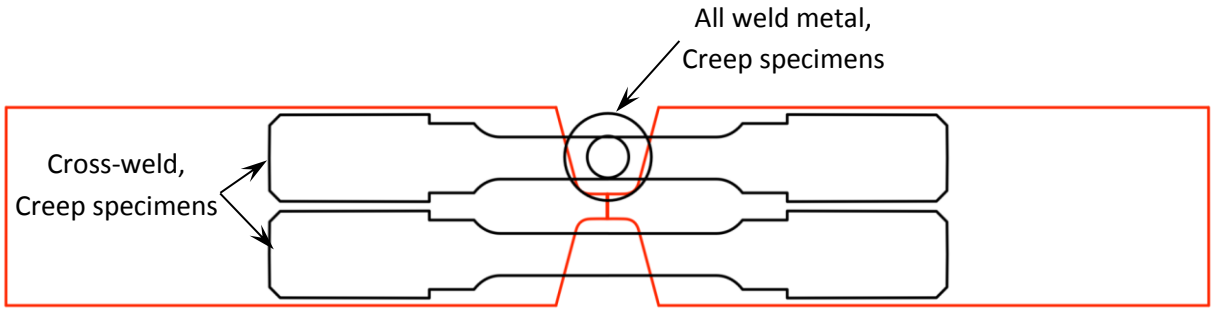

Figure 1. Schematic of the weld joint design to be used for the rest of this project. Schematics of where the creep specimen, cross weld and all-weld metal specimens, will be taken are super-imposed on the weld.

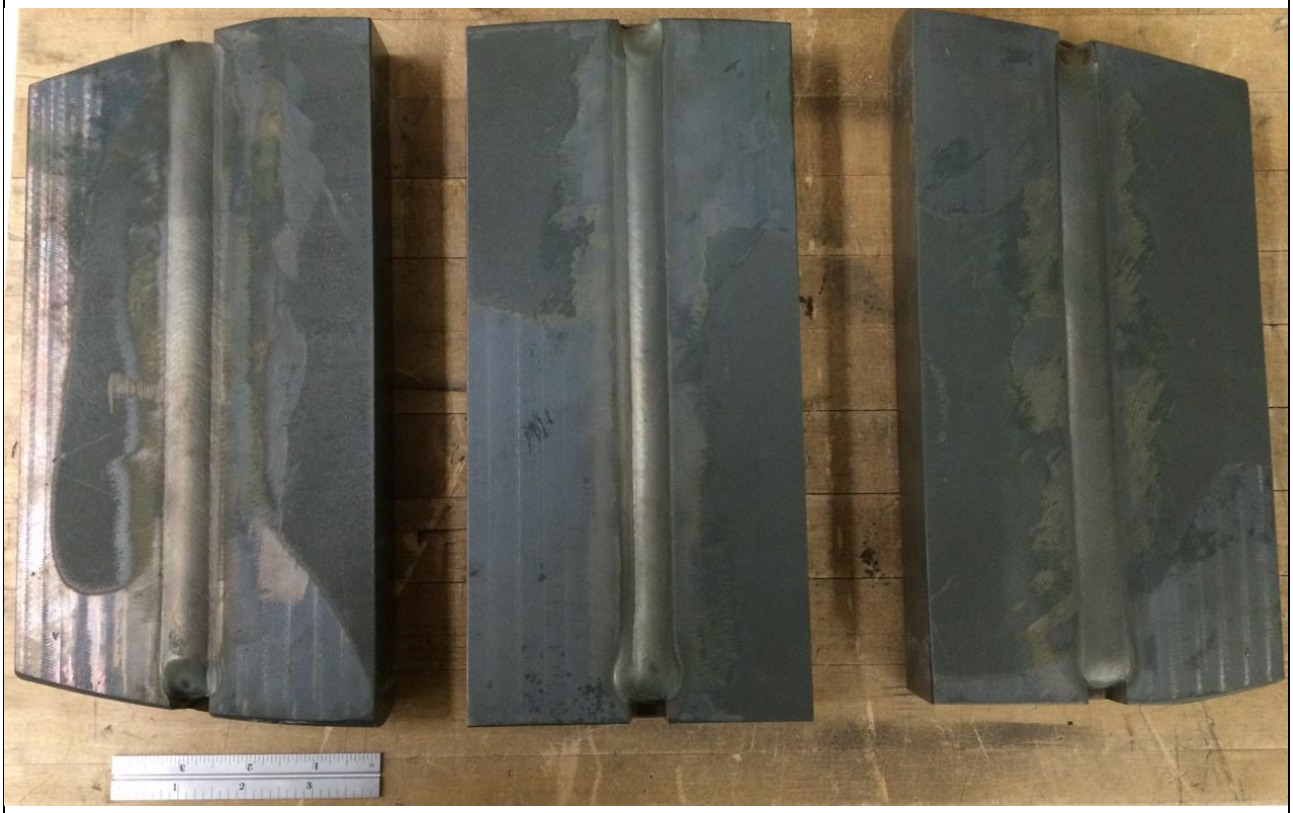

Figure 2. Photograph of the three welds completed in July with the groove design shown in Fig. 1.

Creep specimens from the three wide groove welds in Figure 2, in conjunction with the creep samples made from the remnants of the plate with the initial narrow groove weld for the initial weld qualification effort, will be used in creep testing. The preliminary long term, validation creep test matrix is shown in

Table 1 and the shorter term creep tests for modeling development are shown in Table 2. The creep testing parameters are based on the Larson-Miller plot for welds in Alloy 740H obtained from the Special Metals Datasheet. The long term creep validation tests at 750 and 800ºC were started in the 4th quarter and are expected to run a little over a year.

Table 1. Long term Creep Tests

Test temperature, °C	Specimen ID	Initial Stress, MPa	Orientation	Expected rupture life, hrs	Expected Start date	Expected Finish date	Comments
700		214	Cross weld	9700			Optional – based on creep frame availability
750	740-Q1-9	141	Cross weld	9700	8/22/2016	10/8/2017	Long term
800	740-Q1-7	83	Cross weld	9700	8/22/2016	10/8/2017	Long term

Table 2. Short term creep testing parameters for modeling development

Specimen ID	**Test temperature, °C**	**Test type**	**Initial Stress, MPa**	**Orientation**	**Expected rupture life, hrs**	**Start date**	**Finish date**	**Rupture life, Hrs**
740-Q1-1	700	Rupt	413	CW*	200	8/24/2016	9/21/2016	639
	700	Rupt	400	CW	500			
	700	Rupt	344	CW	1000			
740-Q1-3	750	Rupt	350	CW	200	9/29/2016	10/07/2016	
	750	Rupt	248	CW	500			
	750	Rupt	213	CW	1000			
	800	Rupt	193	CW	200			
	800	Rupt	144	CW	500			
	800	Rupt	138	CW	1000			
	700	Rupt	400	AWM**	500			
	750	Rupt	248	AWM	500			
	800	Rupt	144	AWM	500			

* CW = Cross weld

** AWM = All Weld Metal

One of the short term creep tests in Table 2 has finished (Specimen ID 740-Q1-1) and the creep curve associated with this specimen is shown in Figure 3. The elongation to failure is quite low, <3%, and the fracture in the gage section is being prepared for metallographic observation to evaluate the failure mechanism. The rupture life is considerably longer (>3x) than predicted by the Larson-Miller plot *for welds* from Special Metals, although considerable specimen-to-specimen variation in the creep life can be expected. The creep life lies closer to that predicted for base metal (~1000 hrs). Therefore, the creep stress for the second test, 740-Q1-3 which is being carried out at 750ºC, was based on the Larson-Miller plot for ***base metal***. The initial creep stress in Table 2 for subsequent creep tests will be adjusted based on the creep life of the second test, 740-Q1-3, so that the creep test durations will be closer to that expected in Table 2 and so that all the necessary tests can be completed within the project schedule.

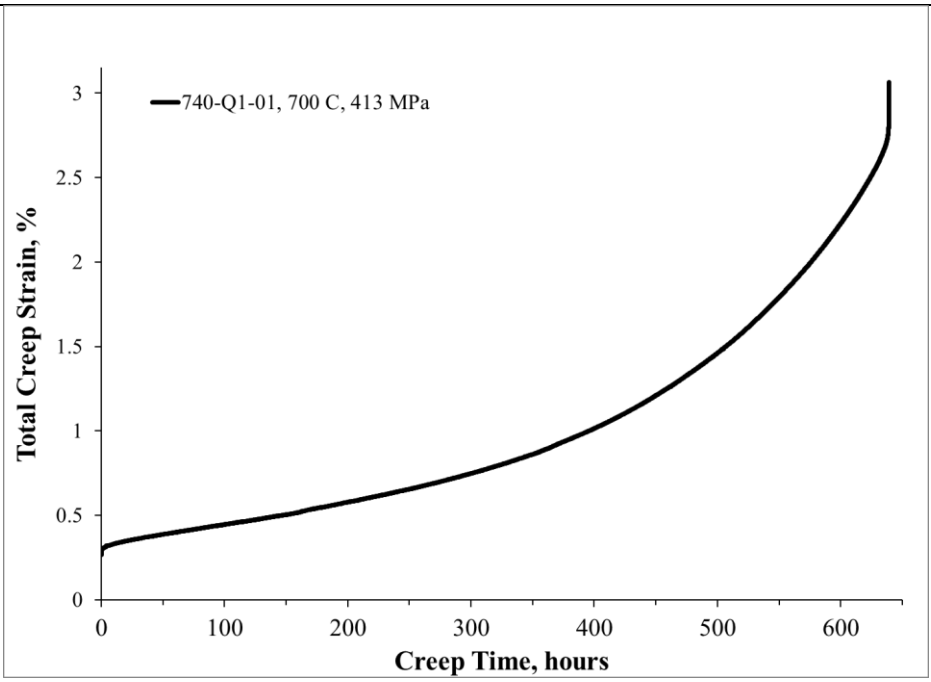

Figure 3. Creep curve for a cross weld creep specimen, 700°C, 413 MPa.

Milestone E, "Characterize Alloy 740H welds"

Remnant material from the narrow groove ASME qualification weld was sectioned and prepared for characterization of the weld microstructure using EBSD. Figure 4 shows a schematic of the planes in the weld that were analyzed. Figure 5a shows the grain orientation map from the transverse section of the upper part of the weld while Figure 5b and c show grain orientation maps for the longitudinal z-direction (looking down on the weld) and the longitudinal y-direction (looking at the side of the weld).

The base metal at either side of Figure 5a is relatively fine-grained and equiaxed. The weld metal is highly elongated due to heat flow during soldification. Where these grains intersect the longitudinal z-plane, Figure 5b, they are relatively equiaxed although much larger than the grains in the base metal. Considerable texturing is evident in both Figure 5a and b. Individual weld passes are clearly evident in the longitudinal y-plane, Figure 5c, with an individual pass depositing about 2.5 mm of material.

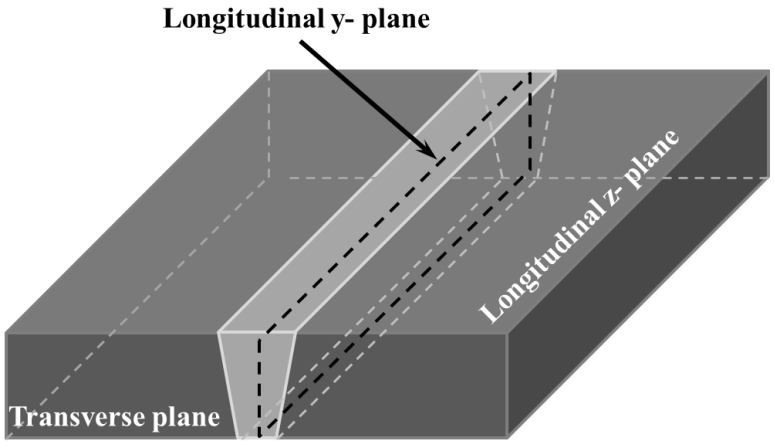

Figure 4. Schematic of analysis planes.

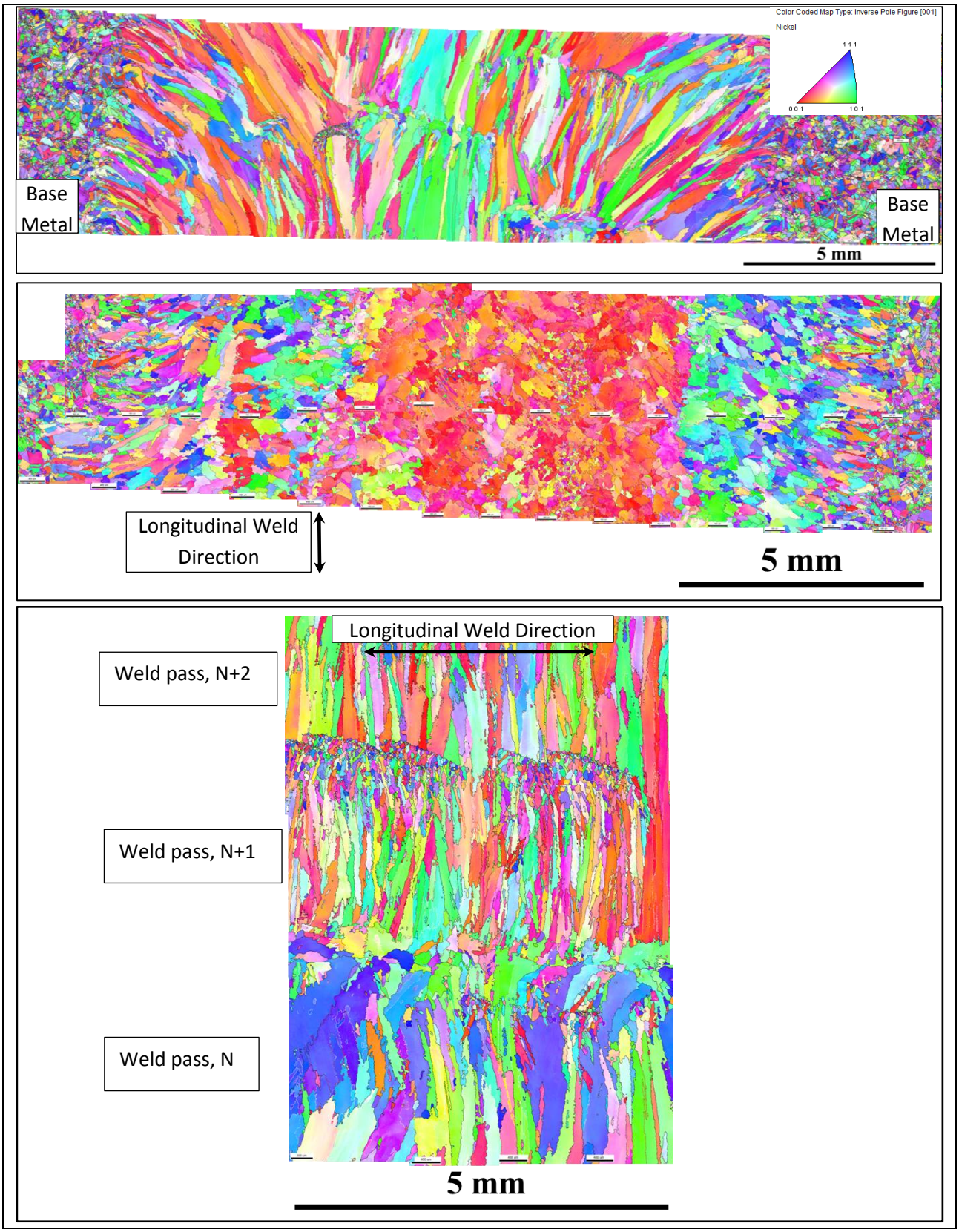
Color Coded Map Type: Inverse Pole Figure [001]
Nickel
1 1 1
0 0 1
1 0 1
Base Metal
Base Metal
5 mm
Longitudinal Weld Direction
5 mm
Longitudinal Weld Direction
Weld pass, N+2
Weld pass, N+1
Weld pass, N
5 mm

Figure 5. Grain orientation maps from the EBSD analysis of (a) the transverse section through the weld, (b) longitudinal z-plane (i.e. looking down on the weld) and (c) longitudinal y-plane (i.e. side view of the weld).

Quantitative information concerning the orientation distribution and grain size distribution as well as the aspect ratio of the grains will be determined using the OIM software which will then be used in the modeling and simulation effort.

Milestone F, "Creep model development – Stage 1"

During the third quarter, the equations governing dislocation climb were developed and incorporated into the developing creep model. The climb rate is dependent on the vacancy concentration. From the 3rd quarter report:

"The vacancy concentration in the matrix is evolved following

$$\dot{c} = -\nabla j + \sum \left(\rho_M^\alpha + \rho_I^\alpha \right) b v_c^\alpha \qquad (13)$$

where *j* is the vacancy flux and the second term is due to the cumulative effect of vacancy absorption or emission to cause climb. It is assumed in Eq. (13) that if climb is occurs on 2 slip systems at the same rate where one acts as source and the other as sink, the net vacancy concentration in the bulk is preserved."

The focus during the 4th quarter was to develop the equations governing the vacancy concentration which determines the dislocation climb rate.

1. Polycrystalline creep model

Polycrystalline-scale creep model based on [1] is developed in this work. The vacancy diffusion will be coupled with our crystal plasticity model to calculate the vacancy rate for dislocation climb. The evolution of vacancy concentration is based on the substitutional motion of atoms and is represented by

$$\dot{c}_v = -\frac{\partial j_i}{\partial x_i} \qquad (1)$$

where c_v is the vacancy concentration, j_i are the flux components along directions i = 1, 2 and 3. The vacancy flux evolves following the Onsager's relation

$$j_i = - L_{ij} \frac{\P m}{\P x_j} \qquad (2)$$

where L_{ij} is the mobility and μ is the chemical potential. The chemical potential is related to the free-energy of the system (Ψ) that has both a chemical (Ψ_c) and a mechanical (Ψ_m) component. The mechanical contribution is related to the elastic strain energy following

$$\psi_m = \frac{1}{2}\varepsilon_{ij}^e C_{ijkl}\varepsilon_{ij}^e \quad (3)$$

where C_{ijkl} is the 4^{th} order elasticity tensor and the elastic strain (ε_{ij}^e) can be represented by

$$\varepsilon_{ij}^e = \varepsilon_{ij} - \varepsilon_{ij}^v - \varepsilon_{ij}^{cr} \quad (4)$$

In Eq.4, ε_{ij} is the total strain, ε_{ij}^{cr} is the inelastic creep strain and ε_{ij}^v is the relaxation strain due to vacancies. A concentration dependent relaxation strain is proposed and follows

$$\varepsilon_{ij}^v = \eta_{ij} c_v \quad (5)$$

where η_{ij} is the relaxation tensor. The chemical energy is described using

$$\psi_c = \frac{E_f}{\Omega_0} c_v + \frac{RT}{\Omega_0}(c_v \log c_v + (1 - c_v)\log(1 - c_v)) \quad (6)$$

where the first term is related to the formation energy of vacancies and the second term represents the entropy of mixing. In Eq.6, E_f is the formation energy, Ω_0 is the molar volume, R is the gas constant and T is the absolute temperature. From the total free energy, the stress can be obtained as

$$\sigma_{ij} = \frac{\partial \psi}{\partial \varepsilon_{ij}^e} = C_{ijkl}\varepsilon_{ij}^e \quad (7)$$

and the chemical potential as

$$\mu = \frac{\partial \psi}{\partial c_v} = \frac{E_f}{\Omega_0} + \frac{RT}{\Omega_0}\log\left(\frac{c_v}{1 - c_v}\right) - \eta_{ij}\sigma_{ij} \quad (8)$$

In this model, the vacancy diffusivity and relaxation tensor on the grain boundary (GB) is considered to be anisotropic, while the bulk behavior is isotropic. Since, the GBs act as vacancy source/sink, diffusion is allowed only along the non-normal direction on GBs. This is enforced through the diffusivity tensor (D_{ij}) following

$$D_{ij} = (1 - \phi)D_B\delta_{ij} + \phi D_{GB}(\delta_{ij} - n_i n_j) \quad (9)$$

where ϕ is the GB phase parameter, which is 0 in the bulk and 1 on GB; D_B and D_{GB} are the bulk and GB diffusivities, respectively and n_i is the GB normal. The mobility is then represented as

$$L_{ij} = \frac{\Omega_0}{RT} c_v(1 - c_v)D_{ij} \quad (10)$$

The relaxation tensor is modified accordingly,

$$\eta_{ij} = (1 - f)\eta_B\delta_{ij} + f\eta_{GB}n_i n_j \quad (11)$$

wherein the relaxation due to the presence of vacancies is assumed only along the GB normal direction.

In the model, the creep strain due to vacancy diffusion is obtained from the material velocity due to their directional substitution with vacancies. Assuming, that the number of substitutional sites remain approximately constant, the creep strain rate is derived as

$$\dot{\varepsilon}_{ij}^{cr} = -(\frac{1}{2}(\frac{\partial j_j}{\partial x_i} + \frac{\partial j_i}{\partial x_j}) - \frac{1}{3}\frac{\partial j_k}{\partial x_k}\delta_{ij})(1-\phi) + \phi\eta_{GB}K_{sv}(c_v - c_v^{eq})n_i n_j \quad (12)$$

where K_{sv} is a constant. The first term dominates in the bulk, whereas the second term is due to the addition or deletion of lattice sites in the GB region. The overall form maintains the isochoric nature of the creep process.

2. Example

The model is tested on a square grain with a length of 25 μ*m* as shown in Fig.1. A normal-distribution function is used to define the grain boundary order parameter and is shown in Fig.1b. The grain is loaded in tension on the top face and compression on the right face with a normal traction of 100 MPa. A temperature of 1000^{o}C is used to derive some of the parameters. The rest are obtained from [1]. Assuming, that initially (t = 0) the free energy is zero, the equilibrium concentration is calculated from Eq.**Error! Reference source not found.** as 1.4×10^{-8}. The equilibrium concentration is maintained on the GB using a Dirichlet boundary condition.

Once the biaxial traction is applied, the top and bottom surfaces acts as vacancy sources, while the right and left faces act as sinks. This is due to the increase and decrease of chemical potential due to the tensile and compressive stresses, respectively, on the GB faces (Fig.2). Due to the source/sink nature of the GBs, the concentration of vacancies increase or decrease in the representative volume and is evident from the spatial distribution shown in Fig.2b. The net flux of vacancies towards the top/bottom faces and away from the left/right faces is also observed in Fig.13. The equivalent creep strain is shown in Fig.4. As can be observed, regions near the triple points have larger creep strain and can be due to the multi-directional vacancy fluxes in these regions. The evolution of the volume averaged equivalent creep strain with time is shown in Fig.4b.

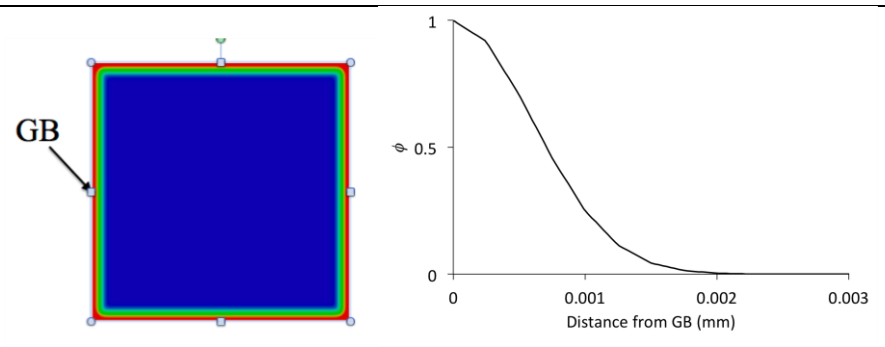

Figure 1: (a) Geometry of the square domain; (b) Grain boundary order parameter.

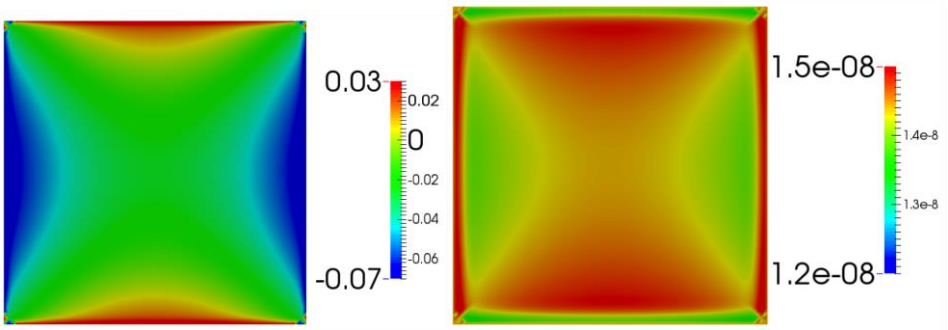

Figure 2: (a) Chemical potential and (b) concentration distribution at t = 100 sec.

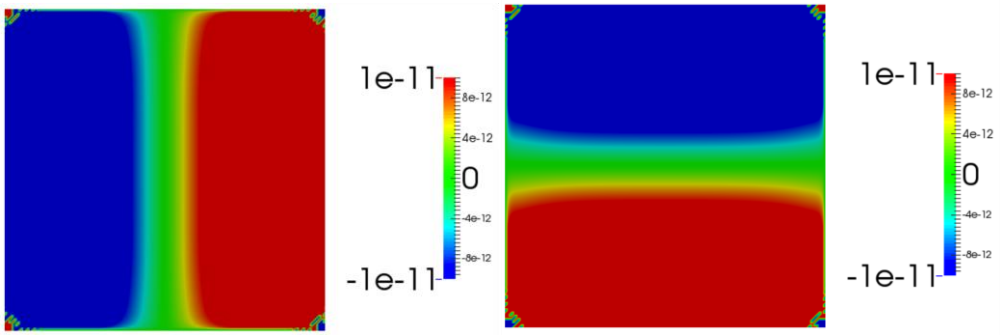

Figure 3: Vacancy flux along (a) x and (b) y directions

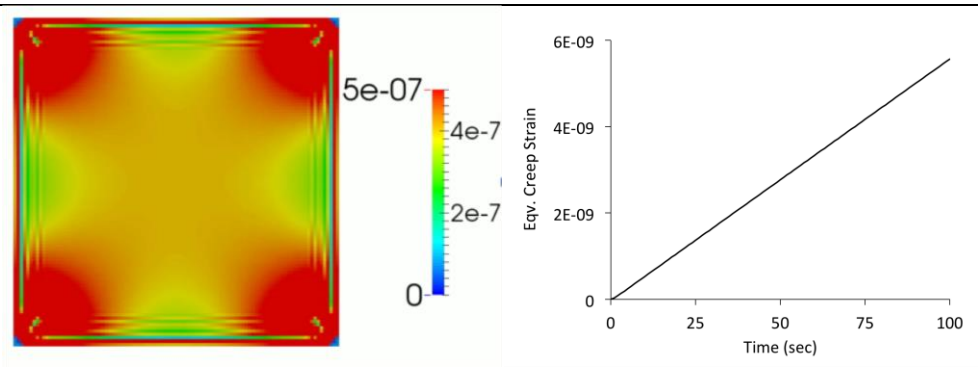

Figure 4: (a) Spatial distribution of equivalent creep strain; (b) Temporal evolution of volume averaged equivalent creep strain.

The existing creep data on Alloy 617 base metal will be used to calibrate the evolving model and produce numerical results in the first quarter of FY17.

References:

[1] A. Villani, E. P. Busso, and S. Forest. Field theory and diffusion creep predictions in polycrystalline aggregates. Modeling and Sim. in Mater. Sci. Eng., 23:055006, 2015.

Other highlights –

- **Aging of Base Metal for Stress Drop Tests:** The effectiveness of γ' particles at pinning mobile dislocations and, thus, imparting creep resistance is dependent on γ' particle size and volume fraction. Stress drop tests are used to evaluate the threshold stress generated by the γ' particle distribution. Long term service can lead to coarsening of the γ' particle distribution and may alter the volume fraction of particles present, both of which alter the threshold stress and, therefore, the creep behavior. In order to accurately model and simulate creep behavior, threshold stress as a function of particle size and volume fraction must be determined. To this end base metal is being aged at 750ºC for 4500 and 8800 hours to generate different γ' particle distributions. The threshold stress for these two particle sizes and the initial post-weld heat treated γ' particle size will be determined. Aging of a sufficient amount of material was begun in the 4th quarter and is scheduled to be removed according the information in Table 3. Again, the goal of this aging treatment is to produce base metal with significantly different γ' particle sizes (and perhaps volume fractions) so that the dependency of the threshold stress on γ' particle size can be determined. This relationship will be used in the simulation of long term creep behavior where the γ' particle size is also coarsening. This data will yield the threshold stress as a function of γ' particle size.

Table 3. Base Metal Aging Information for Stress Drop Tests

Sample ID	Aging Temperature	Target Aging Time, hours	Insertion Date	Expected Removal date
SD-1	750	4500	9/1/2016	3/8/2017
SD-2	750	8800	9/1/2016	9/3/2017

- **γ' Aging Study:** The coarsening behavior/rate of γ' in the base metal and the weld will be evaluated. Inhomogenieties in composition within the weld metal may lead to different volume fractions of γ' particles and coarsening behavior. Weld material is being aged to evaluate coarsening behavior in the weld and base metal at different temperatures. Samples will be aged at different temperatures for various times, Table 4, and then TEM samples will be made to evaluate the γ' size and volume fraction. The 50, 100 and 200 hour aged samples were completed in the fourth quarter.

Table 4. Aging Conditions for γ' Coarsening Study

Aging Temperature, ºC	Aging Time, hrs	Insert Date	Removal Target date	Date/time out	Actual aging hours
650	50	9/6/2016 8:56	9/8/2016 10:56	9/8/2016 10:55	50.0
	100	9/12/2016 9:34	9/14/2016 11:34	9/14/2016 11:30	99.9
	200	9/22/2016 9:35	9/26/2016 13:35	9/26/2016 13:38	200.0
	400	9/29/2016 9:15	10/7/2016 17:15		
	1000				
	3000				
	6000				
	10000				
700	50	9/6/2016 8:56	9/8/2016 10:56	9/8/2016 10:55	50.0
	100	9/12/2016 9:34	9/14/2016 11:34	9/14/2016 11:30	99.9
	200	9/22/2016 9:35	9/26/2016 13:35	9/26/2016 13:38	200.0
	400	9/29/2016 9:15	10/7/2016 17:15		
	1000				
	3000				
	6000				
	10000				
750	50	9/6/2016 8:56	9/8/2016 10:56	9/8/2016 10:56	50.0
	100	9/12/2016 9:34	9/14/2016 11:34	9/14/2016 11:30	99.9
	200	9/22/2016 9:35	9/26/2016 13:35	9/26/2016 13:38	200.0
	400	9/29/2016 9:15	10/7/2016 17:15		

	1000				
	3000				
	6000				
	10000				
800	50	9/6/2016 8:56	9/8/2016 10:56	9/8/2016 10:56	50.0
	100	9/12/2016 9:34	9/14/2016 11:34	9/14/2016 11:30	99.9
	200	9/22/2016 9:35	9/26/2016 13:35	9/26/2016 13:38	200.0
	400	9/29/2016 9:15	10/7/2016 17:15		
	1000				
	3000				
	6000				
	10000				

ISSUES

Approximately $55k is available for carryover into FY17. At present spending rates it is projected that the project can continue for approximately 2 months before current funds are exhausted.

Report Prepared By	Date
Thomas M. Lillo	10/12/2016